



# Cyclic perylene diimide: Selective ligand for tetraplex DNA binding over double stranded DNA

著者	Vasimalla Suresh, Sato Shinobu, Takenaka Fuminori, Kurose Yui, Takenaka Shigeori
journal or publication title	Bioorganic & Medicinal Chemistry
volume	25
number	24
page range	6404-6411
year	2017-10-21
URL	<a href="http://hdl.handle.net/10228/00007414">http://hdl.handle.net/10228/00007414</a>

doi: [info:doi/10.1016/j.bmc.2017.10.014](https://doi.org/10.1016/j.bmc.2017.10.014)



## Cyclic perylene diimide: Selective ligand for tetraplex DNA binding over double stranded DNA

Suresh Vasimalla<sup>a</sup>, Shinobu Sato<sup>a, b</sup>, Fuminori Takenaka<sup>b</sup>, Yui Kurose<sup>b</sup>, Shigeori Takenaka<sup>a, b, \*</sup>

<sup>a</sup> Research Center for Biomicrosensing Technology, Kyushu Institute of Technology, Kitakyushu, Fukuoka 804-8550, Japan

<sup>b</sup> Department of Applied Chemistry, Kyushu Institute of Technology, Kitakyushu, Fukuoka 804-8550, Japan

### ARTICLE INFO

#### Article history:

Received 24 August 2017

Received in revised form 12 October 2017

Accepted 13 October 2017

Available online xxx

#### Keywords:

Cyclic perylene diimide

Tetraplex specific ligand

Human telomere DNA

Basket tetraplex DNA

Inhibition of telomerase activity

### ABSTRACT

Synthesized cyclic perylene diimide, **cPDI**, showed the binding constant of  $6.3 \times 10^6 \text{ M}^{-1}$  with binding number of  $n=2$  with TA-core as a tetraplex DNA in 50mM Tris-HCl buffer (pH=7.4) containing 100mM KCl using Schatchard analysis and showed a higher preference for tetraplex DNA than for double stranded DNA with over  $10^3$  times. CD spectra showed that TA-core induced its antiparallel conformation upon addition of **cPDI** in the absence or presence of  $\text{K}^+$  or  $\text{Na}^+$  ions. The **cPDI** inhibits the telomerase activity with  $\text{IC}_{50}$  of  $0.3 \mu\text{M}$  using TRAP assay which is potential anti-cancer drug with low side effect.

© 2017.

### 1. Introduction

The terminal of DNA in human chromosomes are composed of tandem G-rich d(TTAGGG) repeats up to 2–10kb.<sup>1</sup> These telomeric DNA terminals are a single-stranded 3' overhang having around 100–200 nucleotides. This terminal overhang can form G-quadruplexes by self-associating through Watson-Crick and Hoogsteen hydrogen bonding.<sup>2</sup> Telomeric DNA contains the Shelterin nucleoprotein complex, which protects chromosomal ends from end-to end fusions and DNA damage. Telomerase enzyme adds d(TTAGGG) repeats to the 3' terminus actively and extends the length of telomeric DNA, conforming chromosomal integrity after each cell cycle.<sup>3</sup> Generally, telomerase is up-regulated in 85% of human cancers, and has negligible activity in somatic cells. Thus, for the development of new anticancer drugs and therapeutic applications these guanine-rich sequences have become a very important target.<sup>4</sup> Many approaches have been developed for inhibition of telomerase. Albeit indirect strategy for telomerase inhibition involves the use of small molecules to thermally stabilize G-quadruplex structures formed from these telomeric d(TTAGGG) repeats. The goal of these small molecules is to displace the telomerase and/or other key telomeric proteins such as hPOT1.<sup>5</sup> The potential anti-cancer and therapeutic agents are small molecules that stabilize the G-rich single-strand DNA overhang into G-quadruplex.<sup>6</sup>

During past few years numerous small molecules have been developed to interact with G-quadruplex DNA. Some of these com-

pounds have also established the enzyme telomerase inhibition.<sup>7</sup> Generally G-quadruplex binding ligands are polycyclic, aromatic ligands substituted at multiple positions.<sup>8</sup> In many cases, the selectivity for G-quadruplex DNA over double-stranded DNA of the ligands so far identified is often less than ideal. This low selectivity leads to non-specific cellular cytotoxicity.<sup>9</sup> The major goal for G-quadruplex ligands is to increase the selectivity for G-quadruplex DNA over double-stranded DNA and correspondingly to reduce cytotoxicity in order to use these molecules as telomerase inhibitors, or as biological probes for in vivo detection of G-quadruplex. Therefore it is necessary to understand the mechanism of observed selectivity for G-quadruplex interactive ligands to logically design ligands with improved G-quadruplex selectivity.<sup>10</sup> By using the DOCK shape-complementarity scoring algorithm, previously it has been identified that, 3,4,9,10-perylenetetra-carboxylic acid diimides (PTCDIs) are potential G-quadruplex interactive molecular scaffolds.<sup>11</sup> A perylene diimide PIPER facilitates the formation of G-quadruplex DNA from single-strand DNA<sup>12</sup> as well as certain duplex oligonucleotides. The perylene diimide N,N'-bis(3-(dimethylamino)propyl)-3,4,9,10-perylenetetra-carboxylic acid diimide is found to precipitate in binding trace amounts of calf thymus DNA, providing evidence for double-stranded DNA binding also.<sup>13</sup> These planar, heterocyclic aromatic perylene diimides are known to self-assemble through stacking interactions.<sup>14</sup> Previously reported that this aggregate formation may occur at a nucleation site as in the case of ligands aggregating on DNA templates. In another way, these ligands may also aggregate separately from the DNA in solution, resulting in an aggregate capable of binding DNA or sometimes hiding ligand from ligand-DNA interactions.<sup>15</sup>

\* Corresponding author at: Department of Applied Chemistry, Kyushu Institute of Technology, Kitakyushu, Fukuoka 804-8550, Japan.

Email address: shige@che.kyutech.ac.jp (S. Takenaka)

We have been developing cyclic naphthalene diimide derivatives, where **cNDI** is typical example of this series.<sup>16-20</sup> We found that linker chain of **cNDI** diminished affinity for double stranded DNA keeping binding affinity for tetraplex DNA (Fig. 1). The **cNDI** was more specific for the tetraplex DNA, but the binding affinity has not improved.<sup>16-19</sup> The model perylene diimide PIPER having linear alkyl chain with piperidine as terminal moiety has more binding affinity for tetraplex DNA, but the selectivity over the dsDNA was not improved. In an attempt to further increase the selectivity and affinity of the ligand with tetraplex DNA, in the present work we have synthesized the cyclic perylene diimide which has extended aromatic core compared to naphthalene diimide and the interaction studies of **cPDI** with tetraplex DNA and double stranded DNA were studied. This cyclic chain in perylene diimide prevents the traditional aggregation that takes place in perylene diimides, leading to only the aggregation of two molecules with J-aggregation. Interestingly the **cPDI** has shown the 2-fold improved affinity with the tetraplex DNA and lower affinity with the double stranded DNA by half, emerging it as more efficient anticancer drug.

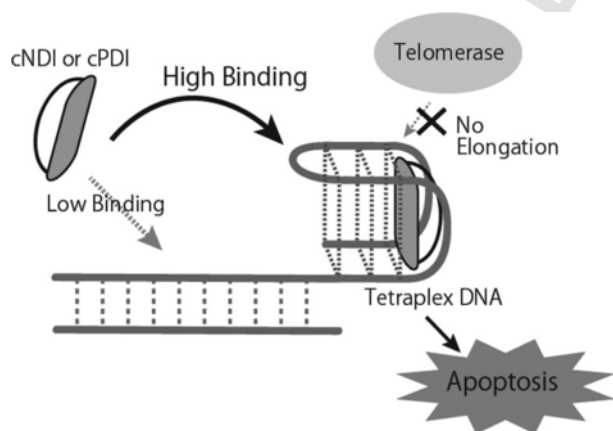
## 2. Material and methods

### 2.1. Reagents

Calf thymus DNA ( $\epsilon$ ,  $12,824\text{M}^{-1}\text{cm}^{-1}$ ),<sup>21</sup> was obtained from Sigma Aldrich (St. Louis, MO). The following oligonucleotides were custom-synthesized from Genenet (Fukuoka, Japan): TA-core; 5'-TAG GGT TAG GGT TAG GGT TAG GG-3' ( $\epsilon$ ,  $236,500\text{M}^{-1}\text{cm}^{-1}$ ), HP-27; 5'-GCG ATT CTC GGC TTT GCC GAG AAT CGC-3' ( $\epsilon$ ,  $245,800\text{M}^{-1}\text{cm}^{-1}$ ), dsOligo; 5'-GGG AGG TTT CGC-3' ( $\epsilon$ ,  $114,000\text{M}^{-1}\text{cm}^{-1}$ ) and 5'-GCG AAA CCT CCC-3' ( $\epsilon$ ,  $108,600\text{M}^{-1}\text{cm}^{-1}$ ). The TA-core, HP-27, ds-oligo were annealed in the measurement buffer before use. The 3.0M Potassium Acetate (pH 5.5), 2.0M KCl, and 5.0M NaCl aqueous solutions were obtained from Life Technologies (Carlsbad, CA). 1.0M Tris-HCl (pH 7.4) buffer was obtained from Sigma-Aldrich (St. Louis, MO).

#### 2.1.1. Synthesis of **cPDI**

**cPDI** was synthesized according to Scheme 1



Scheme 1.

#### 2.1.1.1. *N,N'*-bis{[3-(3-*tert*-Butoxycarbonylamino)propyl]-piperazin-1-yl}propyl} perylene-3,4,9,10-tetracarboxylic acid diimide (**PDI-p-Boc**)

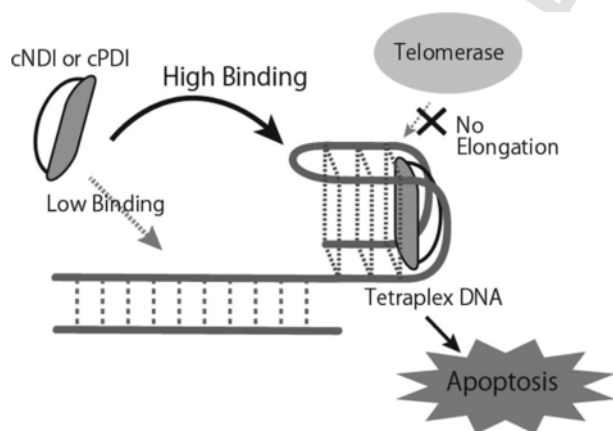
{3-[4-(3-Aminopropyl)piperazin-1-yl]propyl}-carbamic acid *tert*-butyl ester (p-NH2(Boc)) was synthesized as described previously.<sup>20</sup> 1.94 g (6.45 mmol) of p-NH2(Boc) and 200 mL of Toluene (Wako Pure Chemical Industry, Ltd., Tokyo, Japan) were added to 3,4,9,10-Perylenetetracarboxylic dianhydride (Tokyo Chemical Industry Co., Ltd., Tokyo, Japan) 1.01 g (2.58 mmol). It was refluxed for 10 h. After allowing cooling to room temperature, the solvent was distilled off with an evaporator to obtain a red solid. To the solid after ultrasonic irradiation for 1 h, suction filtration was carried out. The resulting red solid was dried under vacuum (0.99 g, Yield 77%).

<sup>1</sup>H NMR (500 MHz, CDCl<sub>3</sub>,  $\delta$  ppm) 1.59 (m, 4H), 1.94 (m, 4H), 2.30 (t, 8H), 2.51 (t, 16H), 3.13 (d, 4H), 4.26 (t, 4H), 5.42 (br s, 2H), 8.55 (d, 4H), 8.63 (d, 4H); MALDI-TOFMS (positive mode,  $\alpha$ -cyano-4-hydroxycinnamic acid ( $\alpha$ -CHCA))  $m/z$  = 958.373 (theory for C<sub>54</sub>H<sub>68</sub>N<sub>8</sub>O<sub>8</sub> + H<sup>+</sup> = 958.189).

#### 2.1.1.2. *N,N'*-Bis{[3-(3-Aminopropyl)piperazin-1-yl]propyl}-perylene-3,4,9,10-tetracarboxylic acid diimide (**PDI-p-NH2**)

In an eggplant flask, PDI-p-Boc 0.176 g (0.184 mmol) and 10 mL dichloromethane (Wako Pure Chemical Industry, Ltd.) was added and dissolved therein, and 5 mL (65.3 mmol) of trifluoroacetic acid (TFA, Wako Pure Chemical Industry, Ltd.) was added to it. It was stirred for 3 h at room temperature. Then the reaction mixture was evaporated under reduced pressure to obtain a dark red solid. This solid was dissolved in small amount of dichloromethane and added

Fig. 1. Strategy of G-quartet specific ligand based on cyclic perylene diimide.



dropwise to 500 mL of ethylacetate for reprecipitation. Suction filtration was carried out, and vacuum drying was carried out to obtain product as maroon color solid (0.25 g, Yield, 88%)

<sup>1</sup>H NMR (500 MHz, CDCl<sub>3</sub>, TMS, δ ppm) 1.95 (m, 4H), 2.28 (d, 4H), 2.80 (t, 4H), 3.00 (m, 8H), 3.30–3.50 (m, 20 H), 4.21 (t, 4H), 7.84–7.99 (m, 8H); MALDI-TOFMS (positive mode, α-CHCA) *m/z* = 760.041 (theory for C<sub>44</sub>H<sub>52</sub>N<sub>8</sub>O<sub>4</sub> + H<sup>+</sup> = 757.953).

### 2.1.1.3. Synthesis of **cPDI**

In an eggplant flask, 0.300 g (0.208 mmol) of PDI-p-NH<sub>2</sub>-6 CF<sub>3</sub>COOH, 0.054 g (0.312 mmol) of Pimelic acid (Tokyo Chemical Industry Co., Ltd.) and 0.237 g (0.625 mmol) of HATU (1-[Bis (dimethyl amino) methylene]-1H-1,2,3-triazolo[4,5-*b*]pyridinium-3-oxidhexafluoro phosphate) (Watanabe Chemical Industries, Ltd., Hiroshima, Japan) were dissolved in 200 mL of *N,N'*-dimethylformamide (DMF). Then a solution obtained by dissolving 4 mL of *N,N*-Diisopropylethylamine in 50 mL of DMF was dropped in the above solution through dropping funnel over 1 h with stirring. After 24 h, the stirring was terminated and the solvent was removed with an evaporator. Thereafter, the crude product was purified by silica gel column chromatography (developing solvent: CHCl<sub>3</sub>: MeOH: diethylamine = 10:0.1:0.02) after distilling off the solvent, it was dried under vacuum and the product was collected as a red color solid (9.1 mg, Yield, 5%). The reverse-phase HPLC using an Inertsil ODS-4 column (inner diameter, 5 μm; size, 4.6 × 250 mm<sup>2</sup>, GL Science Inc., Tokyo, Japan) was carried out in a gradient mode at a flow rate of 1.0 mL min<sup>-1</sup>, where the concentration of acetonitrile was changed linearly from 21% to 70% in water containing 0.1% trifluoroacetic acid over 25 min at 40 °C (Fig. S1).

<sup>1</sup>H NMR (500 MHz, CDCl<sub>3</sub>, δ ppm, Fig. S2) 0.88 (t, 2H), 1.15 (m, 8H), 1.86–2.30 (m, 24H), 2.53 (t, 4H), 2.73 (t, 4H), 2.99 (t, 4H), 4.39 (t, 4H), 6.35 (br s, 2h), 8.67 (d, 4H), 8.60 (d, 4H); MALDI-TOFMS (positive mode, α-CHCA, Fig. S3) *m/z* = 882.343 (theory for C<sub>51</sub>H<sub>60</sub>N<sub>8</sub>O<sub>6</sub> + H<sup>+</sup> = 882.464).

### 2.2. UV-vis measurements

Small amount of the 150 μM TA-core or 3 mM-bp Calf Thymus DNA (CT-DNA as dsDNA) in 50 mM Tris-HCl (pH 7.4) containing 0.10 M KCl was added to 5.0 μM **cPDI** in 50 mM Tris-HCl (pH 7.4) containing 0.10 M KCl, and their absorption spectrum change was monitored at 25 °C. The observed spectrum changes at 500 nm were rearranged with Scatchard plot as the following equation,<sup>22</sup>

$$v/L = K(n - v) \quad (1)$$

where *v*, *L*, *n*, and *K* refer to the saturation fraction as the amount of bound ligand per added DNA, amount of unbound ligand, binding number of ligand per one DNA molecule, and binding affinity, respectively. The *K* and *n* values were obtained from Eq. (1), calculated using the *v* and *L* in the different ratio of ligand and DNA concentration obtained using the non-linear least-squares method. For dsDNA, *nK* values were obtained using the Benesi-Hildebrand method by using the equation,<sup>23</sup>

$$1/\Delta\text{Abs} = 1/(l\Delta\epsilon[\text{ligand}]) + 1/(nKl\Delta\epsilon[\text{ligand}]) \times (1/\text{DNA})$$

### 2.3. Circular dichroism (CD) measurements

#### 2.3.1. CD spectra measurements

CD spectra of the 1.5 μM TA-core were measured in 50 mM Tris-HCl (pH 7.4) containing 0.10 M KCl at 25 °C, in the presence of 0 μM to 7.5 μM of **cPDI** in case of TA-core and 0 μM to 10 μM in case of CT-DNA, at a scan rate of 50 nm/min, using a Jasco J-820 spectropolarimeter (Tokyo, Japan) with the following conditions: response, 4 s; data interval, 0.2 nm; sensitivity, 100 mdeg; bandwidth, 2 nm; and scan number, 4 times.

#### 2.3.2. *T<sub>m</sub>* measurements

Melting curves of 1.5 μM TA-core at 288 nm was measured in 50 mM Tris-HCl (pH 7.4) containing 20 mM KCl or 20 mM NaCl in the absence or presence of 1.5 μM of **cPDI** using a Jasco J-820 spectrophotometer equipped with a temperature controller with the following condition: response; 100 mdeg, temperature gradient; 60 °C/h, response; 1 s; data collecting interval; 0.5 °C, and bandwidth; 1 nm. Three ml of total volume was used in the cell with 1 cm of light path length.

Melting curves of 1.5 μM dsOligo at 283 nm was measured in 50 mM Tris-HCl (pH 7.4) containing 20 mM KCl in the absence or presence of 1.5 μM of **cPDI**.

### 2.4. Isothermal titration calorimetry (ITC)<sup>16</sup>

TA-cores (10 μM) in 50 mM AcOK-AcOH (pH 5.5) or AcONa-AcOH (pH 5.5) were heated at 95 °C for 10 min and subsequently cooled to 25 °C at 1.0 °C/min before being used for ITC. Binding studies were performed using low volume Nano ITC (TA instruments, USA), with a cell volume of 170 μL, at 25 °C. All solutions were degassed for 10 min before use. For **cPDI**, the sample cell was filled with the 10 μM TA-core in 50 mM AcOK-AcOH (pH 5.5) or AcONa-AcOH (pH 5.5), and 1.96 μL of 100 μM **cPDI** 50 mM AcOK-AcOH (pH 5.5) or AcONa-AcOH (pH 5.5) was added into the thermo stated cell repeatedly using a syringe.

The resulting data were analyzed by independent model using NanoAnalyze software (TA instruments).

### 2.5. Topoisomerase I assay<sup>16</sup>

Typically, 0.025 μg/μL pUC19 plasmid DNA (TAKARA Bio, Tokyo, Japan) was incubated with 0.25 units/μL of human Topoisomerase I (Topo I, TAKARA Bio) enzyme containing 0.01% BSA for 5 min at 37 °C in 1 × Topo I reaction buffer (35 mM Tris-HCl (pH 8.0), 72 mM KCl, 5.0 mM MgCl<sub>2</sub>, 5.0 mM Dithiothreitol, 5.0 mM Spermidine). The appropriate amount of compound **cPDI** was then added and the reaction mixture was incubated for a further 1 h at 37 °C. The reaction was finished by adding 2.0 μL of 10% SDS to reaction mixture (20 μL). Then, 0.5 μL of 20 mg/mL proteinase K was added and incubated for 15 min at 37 °C. After that 100 μL of 1 × TE (10 mM Tris-HCl, 1 mM EDTA, pH 8.0) was added and two subsequent extractions were carried out using following mixtures: one of phenol/chloroform/isoamyl alcohol (25:24:1) and second of phenol/chloroform (24:1). Then remaining aqueous DNA sample was run on an agarose gel (1%) at 18 V for 3.5 h, stained with Gel Star (TAKARA Bio) and photographed.

## 2.6. TRAP assay<sup>16</sup>

A TRAP assay was performed by following published literature using a TRAPeze kit (EMD Millipore) according to the manufacturer's instructions. Lysate protein was treated using the TRAPeze kit's positive-control cell according to the manufacturer's instructions. The telomerase reaction solution (12.5  $\mu$ L) consisted of 20 mM Tris-HCl, pH 8.3; 1.5 mM MgCl<sub>2</sub>; 63 mM KCl; 0.05% Tween 20; 1.0 mM ethyleneglycol-bis( $\beta$ -aminoethyl)-*N,N,N',N'*- tetraacetic acid; 1  $\times$  dNTP mixture; 1  $\times$  TS primer; 1  $\times$  primer mix; 2.0 units of Taq polymerase; 250 cells of the lysate protein. The mixture was added to freshly prepared **cPDI** solutions with the concentration ranging 0, 0.5, 1.0, 3.0, 5.0, 7.0, 10.0, 15.0, 20.0  $\mu$ M. Reactions were run under the following conditions: 1  $\times$  30  $^{\circ}$ C, 1 h; 35  $\times$  (95  $^{\circ}$ C, 1 min, 62  $^{\circ}$ C, 1 min, 72  $^{\circ}$ C, 1 min); 1  $\times$  72  $^{\circ}$ C, 10 min. Gel electrophoresis on 12.5% polyacrylamide prepared in 1.25  $\times$  TBE (111 mM Tris base, 111 mM borate, and 2.5 mM ethylenediaminetetraacetic acid, pH 8.0) was run at 200 V for 1 h in 0.7  $\times$  TBE. After electrophoresis, the gel was stained with 1  $\times$  GelStar<sup>®</sup> Nucleic Acid Stain in 1  $\times$  TBE (89 mM Tris base, 89 mM borate, and 2.0 mM ethylenediaminetetraacetic acid, pH 8.0) for 30 min and photographed. The resulting data were analyzed according to the manufacturer's instructions.

## 3. Results and discussions

### 3.1. Binding affinity of **cPDI** with TA-core and CT-DNA by UV-vis absorption studies

The UV-vis absorption spectra were investigated to obtain the binding constant and the number of binding molecules for the interaction of **cPDI** with different DNA forms such as human telomere (TA-core) and calf thymus DNA (CT-DNA). TA-core (5'-TAG GGT TAG GGT TAG GGT TAG GG-3') was known to form the hybrid-I structure in aqueous solution containing KCl.<sup>25,26</sup> and thus this sequence was used in the binding analysis without any complexity. Fig. 2A, B shows a representative spectrophotometric titration of **cPDI** with human telomeric G-quadruplex DNA (TA-core) in K<sup>+</sup> ion. In order to study the selectivity of ligand, we also investigated the interaction of **cPDI** with dsDNA. It shows the absorption peaks at 500 nm and 550 nm. Addition of increasing amounts of G-quadruplex DNAs (0  $\mu$ M–15.7  $\mu$ M) to **cPDI** showed large hypochromicities (42% at 500 nm) and a significant red shift of 13 nm at 500 nm peak and a hyperchromic shift at 550 nm (55%) was observed. We observed isosbestic points at 510 nm and 520 nm of **cPDI** for G-quadruplex DNAs and duplex DNA, respectively. The presence of isosbestic points indicated the equilibrium between the bound and free ligand. Upon the addition of increasing amounts of dsDNA (0  $\mu$ M–323.4  $\mu$ M) to **cPDI**, larger hypochromic shifts (50%) and very small red shifts (8 nm) at

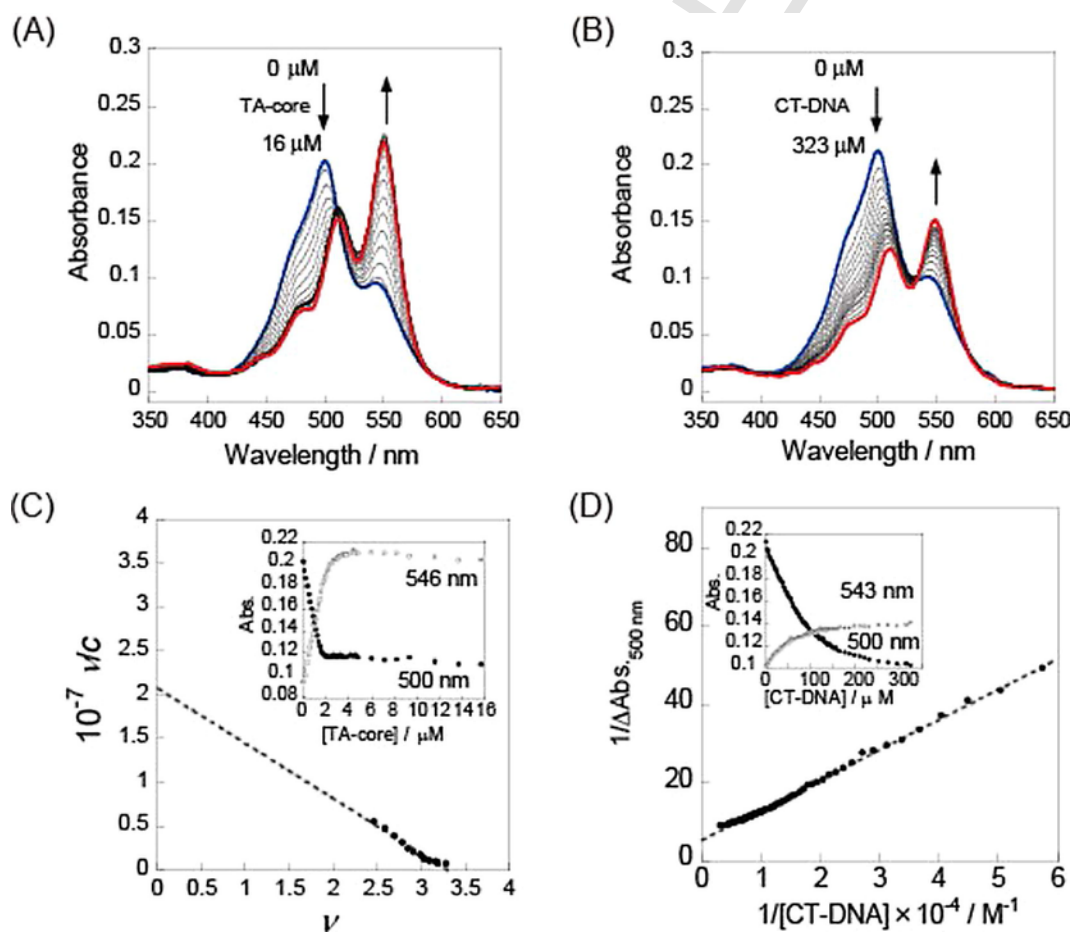


**Fig. 2.** Spectral shifts of **cPDI** on titration with (A) 0  $\mu$ M to 15.7  $\mu$ M of TA-core (B) 0  $\mu$ M to 323.4  $\mu$ M of CT-DNA in 50 mM Tris-HCl (pH 7.4) containing 100 mM KCl. (C) Scatchard plots for binding of **cPDI** to TA-core (D) Benesi-Hildebrand plot for binding of **cPDI** to dsDNA.



500 nm and small hyperchromic shift (29%) at 550 nm were observed. These large changes in the hyperchromic and hypochromic shift with the addition of tetraplex DNA attribute that **cPDI** is effectively binding to TA-core than the CT-DNA suggesting this ligand is not a good dsDNA binder (Fig. 2B). The Scatchard plot representing the binding between **cPDI** and TA-core (KCl) is presented in Fig. 2C. The Scatchard plot was analyzed by the McGhee-von Hippel Scatchard equation<sup>16,22</sup> The solid line in Fig. 2C represents the best fit of the experimental value to the McGhee-von Hippel equation. For dsDNA saturation of binding curves was not achieved, therefore, estimation of K values using the Scatchard equation was impossible. However, nK values were estimated using the Benesi-Hildebrand method (Fig. 2D).<sup>16,23</sup> In the presence of potassium ions **cPDI** binds to TA-core more efficiently than to dsDNA. The intrinsic binding constants (K) of **cPDI** to G-quadruplexes DNA and dsDNA are summarized in Table 1.

### 3.2. CD experiments

Circular dichroism is a typical method to differentiate between different conformations or secondary structures of G-quadruplex DNA. We used circular dichroism to further characterize the binding of the **cPDI** and TA-core quadruplex interaction. As shown in Fig. 3A, after addition of the CD spectrum of TA-core shows hybrid structure with a positive band at 290 nm and a negative band at 240 nm. The G-quadruplex was then titrated with **cPDI**. As shown in Fig. 3B, incremental addition of **cPDI** from 0  $\mu\text{M}$  to 7.5  $\mu\text{M}$  to the quadruplex resulted in large increase in the intensities of negative band at 240 nm and 290 nm in the positive band. However, induced CD signals were observed at 550 nm, which corresponds to the chromophore **cPDI** absorption wavelength. The appearance of induced CD as well as the changes in the positive intensity at 290 nm and negative intensity 240 nm suggests the binding of **cPDI** to this quadruplex and stabilization of antiparallel structure of G-quadruplex DNA.<sup>26-28</sup> On the other hand after addition of  $\text{Na}^+$  the TA-core obtained the basket structure. After the addition of **cPDI** from 0  $\mu\text{M}$  to 4.5  $\mu\text{M}$  the structure converted to antiparallel structure (Fig. 3B). When there is no metal, the TA-core with random coil structure also converted to antiparallel structure upon addition of **cPDI** from 0 to 5 equivalents (Fig. 3C). This shows that **cPDI** stabilizes the antiparallel structure of TA-core in all the cases with  $\text{K}^+$ ,  $\text{Na}^+$  and also no metal (Fig. 3E). In contrast to the TA-core, when titrated with ds-oligo from 0  $\mu\text{M}$  to 10  $\mu\text{M}$  with **cPDI**, there is no change in the intensities of the 250 nm positive band and 280 nm negative bands. Moreover we did not observe any induced signal in case of ds-oligo DNA as shown in Fig. 3D. This indicates that the **cPDI** has very low binding affinity towards ds-oligo and selectively bind to the tetraplex DNA.

### 3.3. Thermal stability of DNAs

Thermal stabilization of G-quadruplex DNA and dsDNA in the presence of **cPDI** was studied using DNA melting temperature mea-

surements. Thermal melting of hybrid type telomeric quadruplex DNA (TA-core) and ds-oligo as double stranded DNA were monitored at 288 nm or 283 nm in the presence of  $\text{K}^+$  and  $\text{Na}^+$  (Fig. S4). The  $T_m$  value was observed around 53.0  $^{\circ}\text{C}$  for TA-core without **cPDI** in presence of  $\text{K}^+$ . We observed that the interaction of **cPDI** with telomeric DNA quadruplex enhanced the stability by 21  $^{\circ}\text{C}$  for TA-core (Table 2). In the previously reported literature it has been proven that thermal melting increases after addition of base to oligonucleotides.<sup>16-20</sup> After the addition of a 1-fold **cPDI** concentration, an increase (up to 21  $^{\circ}\text{C}$ ) in thermal stability was observed (Table 2). In presence of  $\text{Na}^+$  the  $T_m$  was 37.5  $^{\circ}\text{C}$  and TA-core found to be stabilized by 14  $^{\circ}\text{C}$ . The  $T_m$  value was observed around 51.0  $^{\circ}\text{C}$  for dsOligo without **cPDI** in presence of  $\text{K}^+$ . After addition of 1-fold, 2-fold and 3-fold **cPDI** the thermal stability of DNA was not changed considerably (Fig. S4, C). As a result the interaction of **cPDI** with TA-core DNA increases the stability significantly where as it has no stabilizing effect on the ds-DNA. These results give emphasis to the fact that **cPDI** selectively stabilizes telomeric quadruplex DNA over dsDNA. In comparison with our previous report,<sup>16-19</sup> compound **cPDI** showed high stabilizing effect where as **cNDI** shown the stabilization effect with  $\Delta T_m$  of 3  $^{\circ}\text{C}$ . According to the above result, we can conclude that **cPDI** preferably stabilizes telomeric quadruplex DNA than ds-Oligo DNA. **cPDI** has more stabilization effect than **cNDI** reported previously indicating that **cPDI** as an efficient ligand for the G-Quadruplex DNA.

### 3.4. Isothermal titration calorimetry (ITC)

Thermodynamic parameters of the interaction between **cPDI** and the TA-core, which is known as a hybrid-type G-quartet structure, were measured by the ITC titration of 100  $\mu\text{M}$  **cPDI** with the 10  $\mu\text{M}$  TA-core in 50 mM AcOK-AcOH (pH 5.5) or 50 mM AcONa-AcOH at 25  $^{\circ}\text{C}$ . In the ITC experiment **cPDI** was interacted with different DNAs such as TA-core and HP-27 (Fig. 4A, B). A small portion of 150  $\mu\text{M}$  **cPDI** in 0.10 M AcONa-AcOH containing 0.10 M NaCl and AcOK-AcOH containing 0.10 M KCl (pH 5.5) was added to the same buffer containing the 10  $\mu\text{M}$  TA-core and all other types of DNAs. Very stable thermal changes were observed in the parameters such as enthalpy, entropy and free energy in **cPDI**. Double stranded DNA has not shown considerable binding interactions as TA-core. All the thermal and binding parameters of **cPDI** with various DNAs have been tabulated in Table 3. The binding ratios of the ligand to tetraplex DNA was 2:1 in the presence of NaCl. The 2:1 ratio observed in the ITC and the UV studies suggested that the stacking of the ligand to the upper and lower G-quartet aromatic planes takes place with the aggregation of ligand in J-aggregation manner.<sup>29</sup> The  $\Delta H$  and  $T\Delta S$  values in the binding process of **cPDI** with a TA-core were  $-6.84 \text{ kcal mol}^{-1}$  and  $1.38 \text{ kcal mol}^{-1}$ , respectively. This suggested the stable complex formation of **cPDI** with TA-core through the additional interaction of their linker chains such as hydrogen bonding. The thermal changes in the presence of both  $\text{Na}^+$  and  $\text{K}^+$  ions are almost same and confirm the formation of stable complex with TA-core. And in both cases there is no evidence of complex formation with HP-27. After addition of  $\text{K}^+$ ,  $\text{Na}^+$  TA-core obtained the hybrid, basket conformations respectively. Upon increasing the addition of **cPDI** in both cases the ligand stabilizes the TA-core to the hybrid conformation. Thus, **cPDI** showed significant contributions of enthalpy and entropy, and might show effective contribution of the  $\pi$ - $\pi$ -stacking interaction and dehydration after complex formation. And it is being formed a stable complex with tetraplex DNA.

**Table 1**  
Comparison of binding constants of **cPDI** and **cNDI** with TA-core and CT-DNA.

Ligand	$10^{-6} \text{ K/M}^{-1}$	
	TA-core <sup>a</sup>	CT-DNA <sup>b</sup>
<b>cPDI</b>	6.3 $\pm$ 0.4	0.007 $\pm$ 0.0001
<b>cNDI</b>	3.7 $\pm$ 0.2	0.039 $\pm$ 0.001

<sup>a</sup> K determined with Scatchard method.

<sup>b</sup> K determined with Benesi-Hildebrand method.

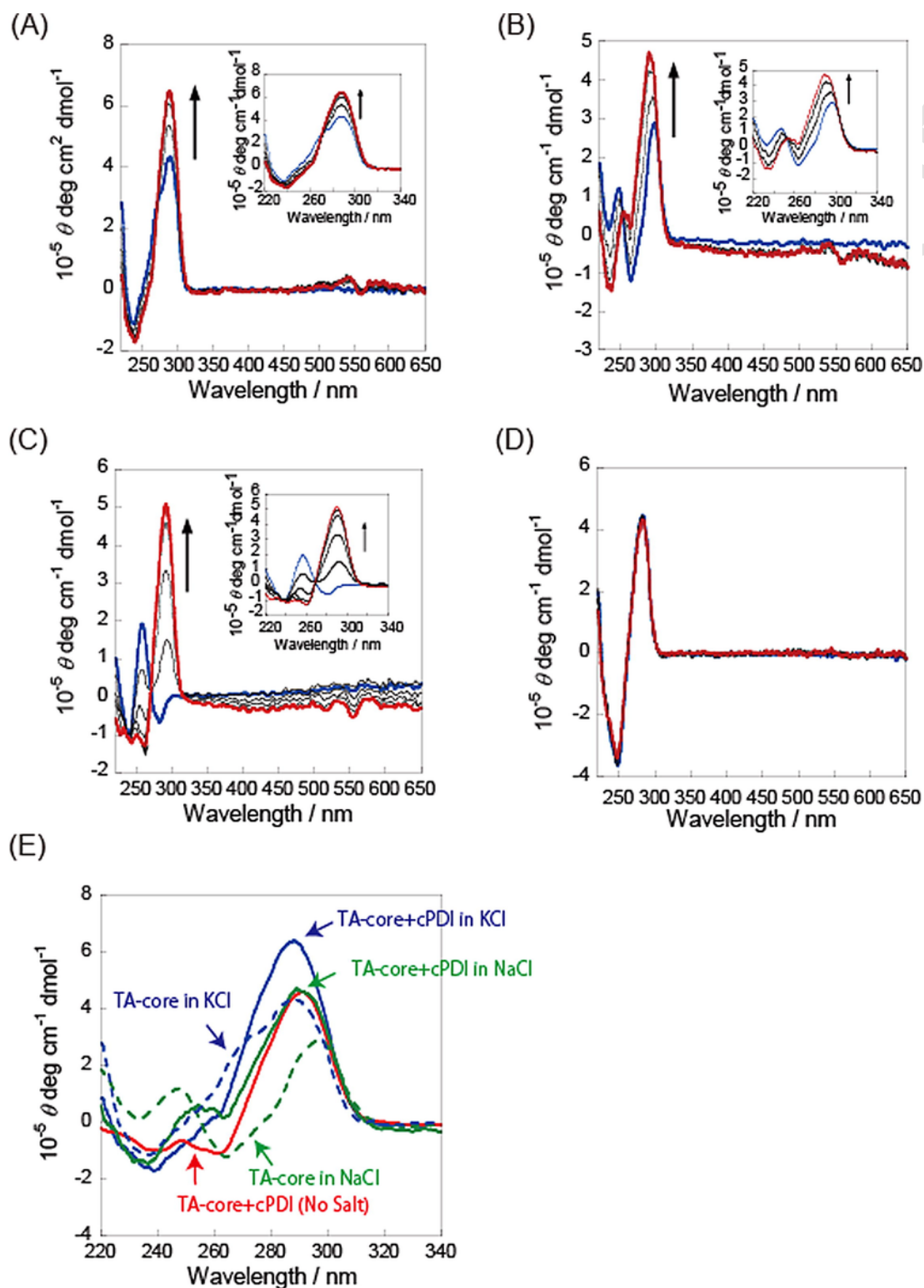


Fig. 3. CD titration of TA-core with cPDI under 50 mM Tris-HCl buffer (pH 7.4) containing (A) 100 mM KCl, (B) 100 mM NaCl, (C) no salt and (D) with CT-DNA.

### 3.5. Topoisomerase I assay

Topoisomerase-based gel assays have been widely used to evaluate compounds for their ability to intercalate into DNA. Cyclic pery-

lene diimide **cPDI** did not show any unwinding of supercoiled plasmid DNA, even using excess amounts of **cPDI** in the Topoisomerase I assay. We could not easily observe supercoiling of plasmid DNA under interactions with **cPDI** over a range of 0  $\mu\text{M}$  to 40  $\mu\text{M}$  (Fig. 5).

**Table 2**  
Melting temperatures of **cPDI** with TA-core and dsOligo.

DNA	Metal cation	T <sub>m</sub>		ΔT <sub>m</sub> /°C <sup>b</sup>
			+ <b>cPDI</b>	
TA-core	K <sup>+</sup>	53.0	74.0	21.0
	Na <sup>+</sup>	37.5	51.5	14.0
dsOligo	K <sup>+</sup>	51.0	50.0	-1.0

<sup>a</sup>1.5 μM TA-core or dsOligo in 50 mM Tris-HCl (pH 7.4) and 20 mM KCl or NaCl.

<sup>b</sup>[**cPDI**]: [DNA]= 1: 1 in 50 mM Tris-HCl (pH 7.4) and 20 mM KCl or NaCl.

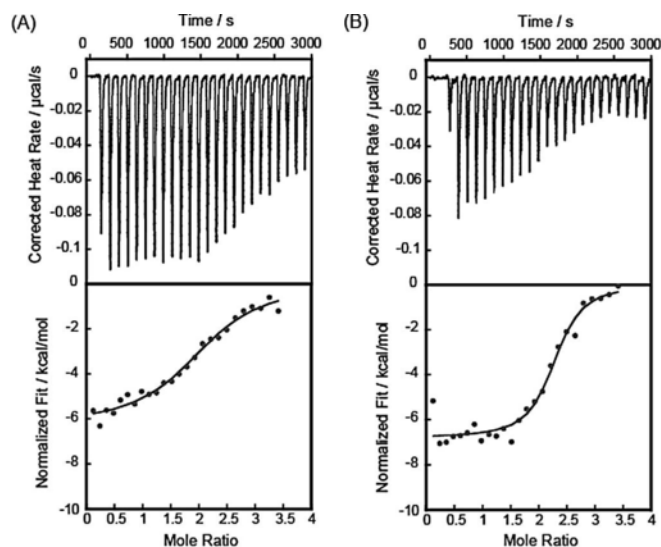


**Fig. 4.** ITC data in the interaction of **cPDI** with TA-core under (A) 50 mM AcOH-AcOK buffer (pH 5.5) and (B) 50 mM AcOH-AcONa buffer (pH 5.5).

**Table 3**  
Binding parameters and of **cPDI** with TA-core and dsDNA in presence of K<sup>+</sup> and Na<sup>+</sup>.

DNA	K <sup>+</sup>		Na <sup>+</sup>	
	TA-Core	HP-27	TA-Core	HP-27
Configuration	Hybrid to antiparallel	Hairpin	Antiparallel	Hairpin
10 <sup>-5</sup> Ka/M <sup>-1</sup>	11.6	–	30.3	–
n	2	–	2	–
ΔH/(kcal/mol)	-6.712	–	-7.141	–
-TΔS/(kcal/mol)	-1.559	–	-1.702	–
ΔG <sub>25°C</sub> /(kcal/mol)	-8.271	–	-8.843	–

–: Not determined.

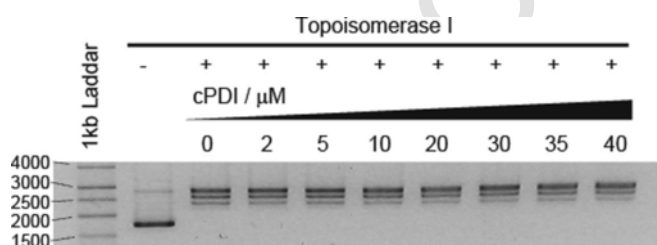


**Fig. 5.** Human topoisomerase I assay.

This clearly indicates that the **cPDI** does not bind to the double stranded DNA.

### 3.6. Evaluation of inhibition of telomerase

After the G-quadruplexes DNA stabilization was recognized for **cPDI**, it is very important to test whether the molecule inhibits telomerase activity or not. To evaluate the ability of **cPDI** to inhibit telomerase, the telomeric repeat amplification protocol (TRAP assay)<sup>30</sup> was carried out using various amounts of **cPDI** (Fig. 6A). The assay clearly shows that **cPDI** is a powerful inhibitor of telomerase with activity in the submicromolar range (IC<sub>50</sub>) 0.24 μM (Fig. 6B). This result suggests that the TS-primer extends the length to form a tetraplex structure and **cPDI** binds to it and stabilizes its structure to inhibit the telomerase reaction. The values obtained from the TRAP assay are comparable to those of previously reported G-quadruplex binding ligands. A number of small ligand have been discovered to inhibit the function of telomerase by stabilizing G-quadruplexes DNA structures.<sup>31</sup> The excellent IC<sub>50</sub> for telomerase inhibition by **cPDI** (0.24 μM) comes from its binding constant. It is suggested that this cyclic perylene diimide compound **cPDI** may deserve biological assays with cancer cell lines to represent a suitable candidate drug which can be used as anticancer drug.

## 4. Conclusions

In conclusion we successfully designed and synthesized a new cyclic perylene diimide ligand **cPDI** and studied the interaction of **cPDI** with tetraplex TA-core DNA and double stranded. The cyclic structure of **cPDI** prevent the traditional aggregation of perylene diimide and favors the formation of J-type aggregation of two **cPDI** molecules in between two successive G-tetrads of G-quadruplex DNA. To estimate the selectivity of the ligand towards tetraplex DNA over the double stranded DNA we performed the binding studies with calf thymus DNA (CT-DNA). The binding studies of **cPDI** have shown that it has shown the binding constant of 6.3 × 10<sup>6</sup> M<sup>-1</sup> with n=2 of binding number with TA-core derived from human telomere DNA sequence and a very low binding constant with double stranded DNA (CT-DNA). All the studies like CD, ITC and T<sub>m</sub> studies were performed in presence of both K<sup>+</sup> and Na<sup>+</sup> ions. From CD it has been observed that in presence and absence of any ion the **cPDI** favors the stabilization of antiparallel structure of TA-core. Thermal changes achieved from ITC experiment confirm **cPDI** forms a stable complex with TA-core. From all the studies it has been proven that **cPDI** does not associate with dsDNA. Moreover, from TRAP assay we found that **cPDI** has the excellent telomere inhibition activity bound to tetraplex DNA generated from TS-primer with telomerase and stabilized to inhibit the telomerase reaction with IC<sub>50</sub> value of 0.24 μM. Our results with **cPDI** as a new class of cyclic ligand, opens a path to design highly selective and efficient ligands for the regulation of the telomerase activity to use as an anticancer drug.

## Uncited references

24,25.

## Acknowledgments

This work was supported in part by JSPS KAKENHI, Grant-in-Aid for Challenging Exploratory Research Grant to S.T. (No. 15K13748).



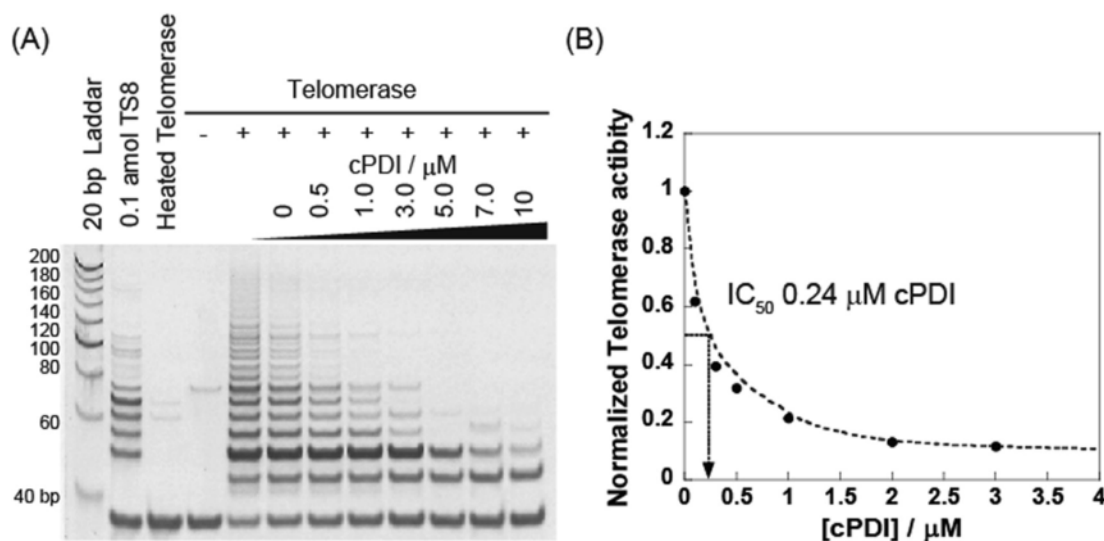


Fig. 6. Gel electropherogram of TRAP assay in the presence of the varied amount of cPDI.

## A. Supplementary data

Supplementary data associated with this article can be found, in the online version, at <https://doi.org/10.1016/j.bmc.2017.10.014>.

## References

1. T. de Lange, V. Lundblad, E.H. Blackburn (Eds.), *Telomeres*, 2nd ed. Cold Spring Harbor Press, New York, NY, 2006.
2. T. Shalaby, G. Fiaschetti, K. Nagasawa, K. Shin-ya, M. Baumgartner, M. Grotzer, G-quadruplexes as potential therapeutic targets for embryonal tumors, *Molecules* 18 (2013) 12500–12537.
3. J.W. Shay, Role of telomeres and telomerase in aging and cancer, *Cancer Discov* 6 (2016) 584–593.
4. J.L. Mergny, C. Helene, G-quadruplex DNA: a target for drug design, *Nat Med* 4 (1998) 1366–1367.
5. A. Arora, N. Kumar, T. Agarwal, S. Maiti, Retraction: human telomeric G-quadruplex: targeting with small molecules, *FEBS J* 277 (2010) 1345–1360.
6. N.W. Luedtke, Targeting G-quadruplex DNA with small molecules, *Chimia* 63 (2009) 134–139.
7. S.M. Kerwin, B. Mamiya, C. Brian, T. Fletcher, J.T. Kern, P.W. Thomas, G-quadruplex DNA as a target for drug discovery: design of telomerase inhibitors based on G-quadruplex DNA structure and dynamics, *Abstr Pap Am Chem Soc* 219 (2000), U6-U6.
8. T.V.T. Le, S. Han, J. Chae, H.J. Park, G-quadruplex binding ligands: from naturally occurring to rationally designed molecules, *Curr Pharm Design* 18 (2012) 1948–1972.
9. S. Neidle, R.J. Harrison, A.P. Reszka, M.A. Read, Structure-activity relationships among guanine-quadruplex telomerase inhibitors, *Pharmacol Therapeut* 85 (2000) 133–139.
10. N.S. Ilyinsky, A.M. Varizhuk, A.D. Beniaminov, M.A. Puzanov, A.K. Shchyolkina, D.N. Kaluzhny, G-quadruplex ligands: mechanisms of anticancer action and target binding, *Mol Biol* 48 (2014) 778–794.
11. T.J.A. Ewing, S. Makino, A.G. Skillman, I.D. Kuntz, DOCK 4.0: search strategies for automated molecular docking of flexible molecule databases, *J Comput Aid Mol Des* 15 (2001) 411–428.
12. O.Y. Fedoroff, M. Salazar, H.Y. Han, V.V. Chemeris, S.M. Kerwin, L.H. Hurley, NMR-based model of a telomerase-inhibiting compound bound to G-quadruplex DNA, *Biochemistry* 37 (1998) 12367–12374.
13. Z.R. Liu, R.L. Rill, N. N'-bis[3,3'-(dimethylamino)propylamine]-3,4,9,10-perylene-tetracarboxylic diimide, a dicationic perylene dye for rapid precipitation and quantitation of trace amounts of DNA, *Anal Biochem* 236 (1996) 139–145.
14. K. Balakrishnan, A. Datar, T. Naddo, et al., Effect of side-chain substituents on self-assembly of perylene diimide molecules: morphology control, *J Am Chem Soc* 128 (2006) 7390–7398.
15. S.M. Kerwin, G. Chen, J.T. Kern, P.W. Thomas, Perylene diimide G-quadruplex DNA binding selectivity is mediated by ligand aggregation, *Bioorg Med Chem Lett* 12 (2002) 447–450.
16. K. Ohtsuka, K. Komizo, S. Takenaka, Synthesis and DNA binding behavior of a naphthalene diimide derivative carrying two dicobalt hexacarbonyl complexes as an infrared DNA probe, *J Organomet Chem* 695 (2010) 1281–1286.
17. M.M. Islam, S. Sato, S. Shinozaki, S. Takenaka, Cyclic ferrocenylnaphthalene diimide derivative as a new class of G-quadruplex DNA binding ligand, *Bioorg Med Chem Lett* 27 (2017) 329–335.
18. S. Sato, S. Takenaka, Ferrocenyl naphthalene diimides as tetraplex DNA binders, *J Inorg Biochem* 167 (2017) 21–26.
19. Y. Esaki, M.M. Islam, S. Fujii, S. Sato, S. Takenaka, Design of tetraplex specific ligands: cyclic naphthalene diimide, *Chem Commun* 50 (2014) 5967–5969.
20. S. Sato, S. Takenaka, Linker effect of ferrocenylnaphthalene diimide ligands in the interaction with double stranded DNA, *J Organomet Chem* 693 (2008) 1177–1185.
21. W. Muller, F. Gautier, Interactions of heteroaromatic compounds with nucleic acids. A - T-specific non-intercalating DNA ligands, *Eur J Biochem* 54 (1975) 385–394.
22. J.D. McGhee, P.H. von Hippel, Theoretical aspects of DNA-protein interactions: co-operative and non-co-operative binding of large ligands to a one-dimensional homogeneous lattice, *J Mol Biol* 86 (1974) 469–489.
23. H.A. Benesi, J.H. Hildbrand, A spectrophotometric investigation of the interaction of iodine with aromatic hydrocarbons, *J Am Chem Soc* 71 (1949) 2703–2707.
24. K.N. Luu, A.T. Phan, V. Kuryavyi, L. Lacroix, D.J. Patel, Structure of the human telomere in  $\text{K}^+$  solution: an intramolecular (3 + 1) G-quadruplex scaffold, *J Am Chem Soc* 128 (2006) 9963–9970.
25. M.H. Li, Z.F. Wang, M.H. Kuo, S.T. Hsu, T.C. Chang, Unfolding kinetics of human telomeric G-quadruplexes studied by NMR spectroscopy, *J Phys Chem B* 118 (2014) 931–936.
26. L. Martino, B. Pagano, I. Fotticchia, S. Neidle, C. Giancola, Shedding light on the interaction between TMPyP4 and human telomeric quadruplexes, *J Phys Chem B* 113 (2009) 14779–14786.
27. E.M. Rezler, J. Seenisamy, S. Bashyam, et al., Telomestatin and diseleno saphyrin bind selectively to two different forms of the human telomeric G-quadruplex structure, *J Am Chem Soc* 127 (2005) 9439–9447.
28. C.C. Chang, C.W. Chien, Y.H. Lin, C.C. Kang, T.C. Chang, Investigation of spectral conversion of d(TTAGGG)<sub>4</sub> and d(TTAGGG)<sub>13</sub> upon potassium titration by a G-quadruplex recognizer BMVC molecule, *Nucleic Acids Res* 35 (2007) 2846–2860.
29. F. Wurthner, T.E. Kaiser, C.R. Saha-Moller, J-aggregates: from serendipitous discovery to supramolecular engineering of functional dye materials, *Angew Chem Int Ed* 50 (2011) 3376–3410.
30. N.W. Kim, M.A. Piatyszek, K.R. Prowse, et al., Specific association of human telomerase activity with immortal cells and cancer, *Science* 266 (1994) 2011–2015.
31. A. De Cian, G. Cristofari, P. Reichenbach, et al., Reevaluation of telomerase inhibition by quadruplex ligands and their mechanisms of action, *Proc Natl Acad Sci USA* 104 (2007) 17347–17352.